

Contribution from the Departments of Chemistry, University of New Brunswick, Fredericton, New Brunswick, Canada E3B 6E2, and Dalhousie University, Halifax, Nova Scotia, Canada B3H 4J3, and AT&T Bell Laboratories, Murray Hill, New Jersey 07974-2070

## X-ray Crystal Structures of the 1,3,2-Benzodithiazolyl Dimer and 1,3,2-Benzodithiazolium Chloride Sulfur Dioxide Solvate: Comparison of the Molecular and Electronic Structures of the 10- $\pi$ -Electron $C_6H_4S_2N^+$ Cation and the $C_6H_4S_2N^\bullet$ Radical and Dimer and a Study of the Variable-Temperature Magnetic Behavior of the Radical

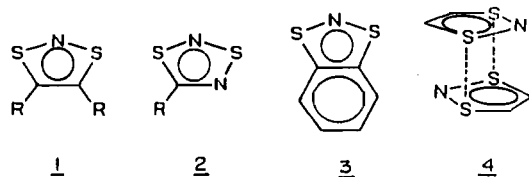
Edward G. Awere,<sup>1a</sup> Neil Burford,<sup>1a,b</sup> Robert C. Haddon,<sup>1c</sup> Simon Parsons,<sup>1a</sup> Jack Passmore,<sup>\*,1a</sup> J. V. Waszczak,<sup>1c</sup> and Peter S. White<sup>\*,1a,d</sup>

Received February 27, 1990

The X-ray crystal structures of the 1,3,2-benzodithiazolyl dimer,  $(C_6H_4S_2N)_2 [(3^*)_2]$ , and 1,3,2-benzodithiazolium chloride sulfur dioxide solvate,  $C_6H_4S_2N^+Cl^-SO_2$ , are reported. Crystal data:  $C_6H_4S_2N^+Cl^-SO_2$ , orthorhombic, space group  $Pnma$ ,  $a = 7.9765$  (6) Å,  $b = 8.8471$  (6) Å,  $c = 13.6309$  (8) Å,  $V = 961.9$  (2), Å<sup>3</sup>,  $Z = 4$ ;  $C_6H_4S_2N^\bullet$ , orthorhombic, space group  $Pbca$ ,  $a = 7.6929$  (3) Å,  $b = 16.0396$  (7) Å,  $c = 10.3863$  (5), Å,  $V = 1281.6$  (2) Å<sup>3</sup>,  $Z = 8$ . The structures were solved by MULTAN-80 and were refined to final  $R$  values of 0.040 and 0.030, respectively. The crystal structure of  $C_6H_4S_2N^+Cl^-SO_2$  consists of discrete, planar cationic units, chloride anions, and  $SO_2$  molecules, with significant contacts between the anion and the  $SO_2$  molecule, implying some  $(SO_2Cl^-)_n$  character, and the sulfur centers of the cation, giving a two-dimensional polymeric macrostructure. The centrosymmetric 1,3,2-benzodithiazolyl dimer contains two  $C_6H_4S_2N$  units joined by two long S-S bonds [3.175 (1) Å], with interplanar spacing of 3.0 Å between the two  $C_6S_2$  mean planes. The  $C_6S_2$  segment of the monomeric unit is planar with the nitrogen atom displaced by 0.186 (2) Å above this plane away from the center of symmetry. The dimers are linked by very weak S...S contacts [3.477 (1), 3.781 (1) Å] into a sheetlike infinite two-dimensional net. Variable-temperature magnetic susceptibility measurements show the solid to be essentially diamagnetic, but on melting the compound becomes paramagnetic ( $\mu(87^\circ C) = 1.54 \mu_B$ ). On this basis  $C_6H_4S_2N^\bullet$  is classified as a *paramagnetic liquid*. The electronic structures of the radical/cation systems  $C_6H_4S_2N$  and HCSNSCH are examined at the ab initio STO-3G level and differences in the experimental geometries of the corresponding cations accounted for.  $C_6H_4S_2N^+$  is shown to be a heteronaphthalenic system, and all the structural differences between the radical and cation are completely rationalized in terms of the nature of the SOMO of  $3^*$ , which is based primarily, but not exclusively, on the SNS region of the molecule. The dimeric structure of  $(3^*)_2$  is modeled by CNDO/2 calculations on  $(HCSNSCH)_2$ , and  $(3^*)_2$  is classified as a  $\pi^*-\pi^*$  dimer of radical monomers. Distortions from planarity of  $3^*$  within  $(3^*)_2$  are rationalized by relative energy calculations, which imply easy deformation of the SNS moiety.

### Introduction

We have recently reported the preparation, isolation, and characterization of derivatives of the SNS-containing radical systems  $1^\bullet$  ( $R = CF_3$ ) and  $2^\bullet$  ( $R = Me, tBu$ ).<sup>2</sup> In addition to



their novel stability, these compounds exhibit a variety of unusual physical and chemical properties. For example, at room temperature they are monomeric liquids, and as such, we refer to them as *paramagnetic liquids*.<sup>2b</sup> In addition, all derivatives of  $2^\bullet$  ( $R = CF_3, CH_3, tBu, I, NMe_2$ ) investigated undergo highly specific, essentially quantitative, photochemically induced rearrangements to the thermodynamically favored disulfide isomer RCN $\overline{SSN}$ .<sup>3</sup>

These, and related compounds,<sup>4</sup> may also prove to be of interest in the solid state, as precursors for charge-transfer complexes leading to synthetic metals,<sup>5</sup> and this possibility is currently under investigation in the case of  $(C_6H_4S_2N^+)_2 (3^*)_2$ .<sup>6</sup> A comprehensive understanding of these systems was hindered by the lack of structural information. The low melting points of these compounds (liquids at room temperature) made structural information difficult to obtain, and this motivated us to examine the structure of the benzo derivative  $(3^*)_2$  (mp 85–87 °C), originally identified in dilute solution by Sutcliffe<sup>7</sup> and isolated on a preparative scale by Wolmershäuser.<sup>4a</sup> Variable-temperature magnetic susceptibility measurements show that the golden colored  $(3^*)_2$  solid is essentially diamagnetic, but the liquid is paramagnetic, consistent with the behavior of  $1^\bullet$  ( $R = CF_3$ ),  $2^\bullet$  ( $R = Me, tBu$ ),<sup>2</sup> and other related radicals.<sup>3</sup> We also report the X-ray crystal structure of  $C_6H_4S_2N^+Cl^-SO_2$  ( $3^+Cl^-SO_2$ ) and the dimer of the radical,  $(3^*)_2$ .

- (1) (a) University of New Brunswick. (b) Dalhousie University. (c) AT&T Bell Laboratories. (d) Present address: Department of Chemistry, The University of North Carolina at Chapel Hill, Chapel Hill, NC 27599-3290.
- (2) (a) Awere, E. G.; Burford, N.; Mailer, C.; Passmore, J.; Schriver, M. J.; White, P. S.; Banister, A. J.; Oberhammer, H.; Sutcliffe, L. H. *J. Chem. Soc., Chem. Commun.* **1987**, 66. Schriver, M. J.; Burford, N.; Passmore, J.; Oberhammer, H.; Englert, U.; Strähle, J. To be published. (b) Brooks, W. V. F.; Burford, N.; Passmore, J.; Schriver, M. J.; Sutcliffe, L. H. *J. Chem. Soc., Chem. Commun.* **1987**, 69. Burford, N.; Passmore, J.; Schriver, M. J.; Strähle, J.; Englert, U.; Oberhammer, H.; Sutcliffe, L. H. To be published. (c) MacLean, G. K.; Passmore, J.; Rao, M. N. S.; Schriver, M. J.; White, P. S. *J. Chem. Soc., Dalton Trans.* **1985**, 1405.
- (3) (a) Burford, N.; Passmore, J.; Schriver, M. J. *J. Chem. Soc., Chem. Commun.* **1986**, 140. (b) Burford, N.; Passmore, J.; and co-workers. Work in progress.

- (4) See for example: (a) Wolmershäuser, G.; Schnauber, M.; Wilhelm, T. *J. Chem. Soc., Chem. Commun.* **1984**, 573. (b) Feher, F.; Malcharek, F.; Glinka, K. Z. *Naturforsch.* **1971**, 26B, 67. (c) Wolmershäuser, G.; Schnauber, M.; Wilhelm, T. *Mol. Cryst. Liq. Cryst.* **1985**, 120, 323. (d) Hayes, P. J.; Oakley, R. T.; Cordes, A. W.; Pennington, W. T. *J. Am. Chem. Soc.* **1985**, 107, 1346. (e) Weinstock, L. M.; Shinkai, I.; Katritzky, A. R.; Rees, C. W. In *Comprehensive Heterocyclic Chemistry*; Pergamon Press: Oxford, England, 1984; Vol. 6/4B, pp 513–543. (f) Atherton, N. M.; Ockwell, J. N.; Dietz, R. J. *Chem. Soc. A* **1967**, 771. Bock, H.; Hanel, P.; Neidlein, R. *Phosphorus Sulfur Relat. Elem.* **1988**, 39, 235. (g) Wolmershäuser, G.; Schnauber, M.; Wilhelm, T.; Sutcliffe, L. H. *Synth. Met.* **1986**, 14, 239. (h) Dormann, E.; Nowak, M. J.; Williams, K. A.; Angus, R. O.; Wudl, F. *J. Am. Chem. Soc.* **1987**, 107, 2594.
- (5) (a) Haddon, R. C. *Nature (London)* **1975**, 256, 394. (b) Haddon, R. C. *Aust. J. Chem.* **1975**, 28, 2343. (c) Candell, E.; Shaik, S. S. *Inorg. Chem.* **1987**, 26, 3797.
- (6) Haddon, R. C.; Chichester, S. V.; Waszczak, J. V.; Awere, E. G.; Passmore, J. Unpublished results.
- (7) Harrison, S. R.; Pilkington, R. S.; Sutcliffe, L. H. *J. Chem. Soc., Faraday Trans.* **1984**, 80, 669.

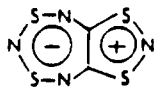
$3^+$  is an isomer of the much investigated Hertz salt,<sup>8a</sup> which contains 1,2,3-benzodithiazolium cations, a derivative of which has been structurally characterized by Bats et al.<sup>8b</sup> The heteronaphthalenic nature of  $3^+$  is supported by a comparison of its electronic structure and geometry with those of naphthalene. The differences in geometries of  $3^+$  and  $1^+$  have been accounted for by a comparison of their electronic structures. The structural differences between  $3^+$  and  $3^*$  (meaningful because of high accuracy in both cases) are completely rationalized by occupation in the radical of the single occupied molecular orbital (SOMO), based mainly, but not exclusively, in the SNS region. The geometry of  $(3^*)_2$  is accounted for by envisaging dimerization of  $3^*$  via overlap of the two radical SOMO's at all four sulfur atoms, and this model is supported by calculations of the electronic structure of **4** as a model for  $(3^*)_2$ . Thus the electronic structures and geometries of  $1^+$ ,  $3^+$ , and  $3^*$  have been accommodated into the conceptual framework of organic chemistry and part of the ground work has been established, on which a complete understanding of the unusual properties of these CSNSC-containing species can be achieved. In addition, they are of interest in the context of the recent preparation and characterization of a wide range of related heteronaphthalenic cations<sup>8c</sup> and the structures and properties of more complex CSNSC-containing ring systems,<sup>8d,e</sup> including benzobis(dithiazole) (BBDTA).<sup>8f</sup> A preliminary account of part of this work has been published.<sup>2a</sup>

### Experimental Section

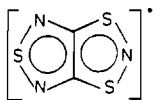
General techniques and apparatus have been described.<sup>9a</sup> Volatile materials were manipulated in a vacuum line ( $10^{-3}$  Torr), and solids, in a Vacuum Atmospheres Dri-Lab equipped with a Dri-Train and an internal circulating drying unit containing 3-Å molecular sieves. Crystals suitable for X-ray analyses were mounted in the Dri-Lab into hand-drawn (0.5 mm) Pyrex capillary tubes predried at 270 °C. ESR spectra were recorded in  $\text{CCl}_3\text{F}$  solutions at  $-70$  °C by using a locally modified version of the Varian E-4 spectrometer fitted with a variable-temperature control unit. DPPH was used as the field marker. IR spectra were obtained as Nujol mulls on CsI plates in the 4000–200- $\text{cm}^{-1}$  region by using a Perkin-Elmer 683 IR spectrometer. Raman spectra were obtained at  $-196$  °C with samples mounted in sealed capillary tubes immersed in an evacuated transparent dewar containing liquid nitrogen with a Spex-Ramalab spectrometer of slit width 4  $\text{cm}^{-1}$  and a Spectra Physics 164-W argon ion green laser (5145 Å) exciting line at 190 mW.

**Preparation, Crystal Growth, and Characterization of  $\text{C}_6\text{H}_4\text{S}_2\text{N}^+\text{Cl}^-\text{SO}_2$  ( $3^+\text{Cl}^-\text{SO}_2$ ) and  $\text{C}_6\text{H}_4\text{S}_2\text{N}^+$  ( $3^+$ ).**  $3^+\text{Cl}^-$  was prepared according to the literature outline (yield 1.14 g, 100%).<sup>4a,b</sup> Details are included with the supplementary material. A solution of  $3^+\text{Cl}^-$  (0.35 g, 1.85 mmol) in  $\text{SO}_2$  (3.25 g) was prepared in one bulb of a two-bulb vessel incorporating

- (8) (a) Warburton, W. K. *Chem. Rev.* **1957**, *57*, 1011. (b) Bats, J. W.; Fuess, H.; Weber, K. L.; Roesky, H. W. *Chem. Ber.* **1988**, *116*, 1751. (c) Burford, N.; Royan, B. W.; Linden, A.; Cameron, T. S. *J. Chem. Soc., Chem. Commun.* **1988**, 842. Burford, N.; Royan, B. W.; Linden, A.; Cameron, T. S. *Inorg. Chem.* **1989**, *28*, 144. Burford, N.; Royan, B. W. *J. Chem. Soc., Chem. Commun.* **1989**, 19. Burford, N.; Royan, B. W. *Phosphorus, Sulfur Silicon Relat. Elem.* **1989**, *41*, 38. Burford, N.; Royan, B. W.; White, P. S. *J. Am. Chem. Soc.* **1989**, *111*, 3746. Burford, N.; Dipchand, A. I.; Royan, B. W.; White, P. S. *Acta Crystallogr.*, in press. (d) For example:



Jones, R.; Morris, J. L.; Rees, C. W.; Williams, D. J. *J. Chem. Soc., Chem. Commun.* **1985**, 654. (e) For example:



Wolmershäuser, G.; Johann, R. *Angew. Chem., Int. Ed. Engl.* **1989**, *28*, 920. (f) Wolmershäuser, G.; Wortmann, G.; Schnauber, M. *J. Chem. Res., Synop.* **1988**, 358.

- (9) (a) Murchie, M.; Passmore, J. *Inorg. Synth.* **1986**, *24*, 76. (b) Apblett, A.; Grein, F.; Johnson, J. P.; Passmore, J.; White, P. S. *Inorg. Chem.* **1986**, *25*, 422.

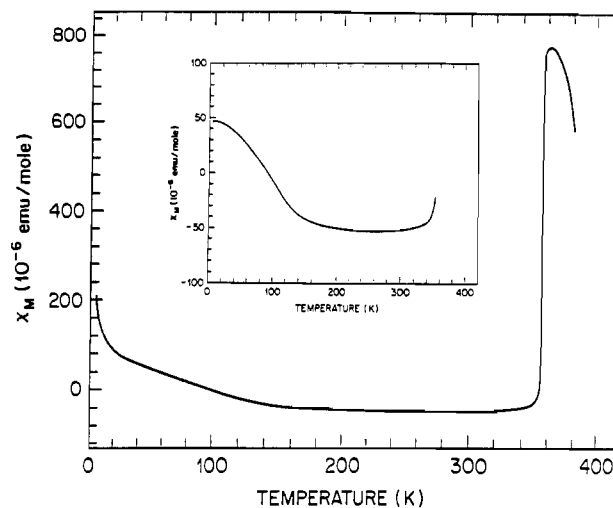


**Figure 1.** Variable-temperature-measured magnetic susceptibility of  $\text{C}_6\text{H}_4\text{S}_2\text{N}^+$ . Inset: Plot after subtraction of the Curie contribution.

a sintered-glass frit and a J. Young Teflon-stemmed valve. The solvent was evaporated into the second bulb, which was cooled to 10 °C by tap water over 3 days to produce long, needlelike, yellow crystals of  $3^+\text{Cl}^-\text{SO}_2$  beneath a yellow solution. The solution was filtered and the solvent removed under dynamic vacuum for 30 min. The crystals were examined under a microscope, carefully cut, and mounted in Pyrex capillaries.<sup>9b</sup> A powdered sample of  $3^+\text{Cl}^-\text{SO}_2$  subjected to dynamic vacuum for 24 h showed no weight loss, and the infrared spectrum was identical with that of the original crystalline compound.

$\text{C}_6\text{H}_4\text{S}_2\text{N}^+$  (0.75 g, 90% recovered yield) was prepared as shiny flakes, according to the literature outline.<sup>4a</sup> Details are included in the supplementary material. Small crystals were grown by vacuum sublimation at 40 °C in a glass tube (300-mm long, 15-mm o.d.) fitted with a J. Young Teflon in glass valve. The crystals are golden or bright golden in incident light, depending on the angle, and black in transmitted light. No color change is evident with long exposure to light. The crystals are malleable and on grinding give flakes having a shiny, lustrous, metallic appearance. They are very sensitive to air, and upon exposure they acquire a copper color and ultimately a green coating.  $\text{C}_6\text{H}_4\text{S}_2\text{N}^+$  has ca. 8, 11, 12, and 13% w/w solubility in  $\text{CCl}_3\text{F}$ ,  $\text{CH}_3\text{CN}$ , *n*-hexane, and benzene, respectively, at room temperature. The solubility decreases with a decrease in temperature.

$\text{C}_6\text{H}_4\text{S}_2\text{N}^+\text{Cl}^-$ : mp/dec pt 216–218 °C; IR (Nujol mull, CsI) 3070 (m), 2970 (w), 1528 (m), 1430 (m), 1423 (m), 1328 (w), 1188 (vw), 1158 (vw), 1078 (w), 947 (w), 776 (vs), 766 (s), 747 (s), 726 (s, sh), 547 (m), 485 (s), 445 (s), 395 (s)  $\text{cm}^{-1}$ ; Raman ( $-196$  °C; areas under peaks in parentheses) 1572 (<9), 1524 (<9), 1423 (53), 1328 (35), 1072 (57), 1052 (17), 1012 (17), 992 (<9), 784 (46), 764 (69), 756 (100), 554 (27), 480 (9), 448 (62), 310 (9)  $\text{cm}^{-1}$ .

$\text{C}_6\text{H}_4\text{S}_2\text{N}^+\text{Cl}^-\text{SO}_2$ : mp/dec pt 129–218 °C; IR (Nujol mull, CsI) 3060 (w), 1528 (m), 1423 (s), 1333 (m), 1295 (vs) [ $\nu_s(\text{SO}_2)$ ], 1276 (sh), 1135 (s), [ $\nu_s(\text{SO}_2)$ ], 1086 (m), 1068 (w), 1058 (w), 1023 (w), 798 (w), 771 (sh), 761 (vs), 721 (sh), 560 (m), 530 (s) [ $\delta(\text{SO}_2)$ ], 480 (s), 445 (s), 396 (m)  $\text{cm}^{-1}$ ; Raman ( $-196$  °C; areas under peaks in parentheses) 1572 (22), 1524 (34), 1424 (37), 1332 (87) [ $\nu_s(\text{SO}_2)$ ], 1244 (23), 1166 (6), 1126 (69) [ $\nu_s(\text{SO}_2)$ ], 1078 (17), 1054 (25), 1016 (14), 948 (12), 796 (22), 778 (<4), 766 (100), 752 (7), 690 (15), 550 (90) [ $\delta(\text{SO}_2)$ ], 543 (<4), 480 (37), 453 (32), 394 (13), 310 (25), 240 (14), 206 (4), 116 (16)  $\text{cm}^{-1}$ .

$\text{C}_6\text{H}_4\text{S}_2\text{N}^+$ : mp 85–87 °C to give initially a golden liquid, which on further heating for 2 min turned bluish black, indicating some decomposition; IR (Nujol mull, CsI) 1433 (m), 1298 (w), 1161 (w), 1098 (w), 1033 (w), 957 (w), 756 (vs), 711 (sh), 701 (vs), 535 (m), 495 (w), 430 (m)  $\text{cm}^{-1}$ ; ESR ( $\text{CFCl}_3$ ,  $-70$  °C)  $g = 2.008 \pm 0.001$ ,  $a^{14\text{N}} = 1.12 \pm 0.01$  mT,  $a^{\text{H}} = 0.06 \pm 0.01$  mT (quintet), essentially the same as that previously reported.<sup>7</sup>

**Magnetic Susceptibility Measurements. Apparatus.** The magnetic susceptibility was measured from 4.2 to 380 K with the Faraday technique. Details of the experiment have been described elsewhere.<sup>10</sup> Low-temperature data were obtained at intervals of about 1 K by using a helium cryostat cooled at an average rate of 1 K/min. The absolute accuracy of the susceptibility is  $\pm 2\%$  as determined by a comparison with several standards. The relative accuracy of these measurements is much higher, approximately  $\pm 0.06\%$ , so that small changes can easily be de-

- (10) DiSalvo, F. J.; Waszczak, J. V. *Phys. Rev.* **1981**, *B23*, 457.

Table I. Crystal Data for 3<sup>+</sup>Cl<sup>-</sup>·SO<sub>2</sub> and 3<sup>+</sup>

formula	C <sub>6</sub> H <sub>4</sub> S <sub>2</sub> N <sup>+</sup> Cl <sup>-</sup> ·SO <sub>2</sub>	C <sub>6</sub> H <sub>4</sub> S <sub>2</sub> N
MW	253.74	154.22
cryst class	orthorhombic	orthorhombic
space group	<i>Pnma</i>	<i>Pbca</i>
<i>a</i> , Å	7.9765 (6)	7.6929 (3)
<i>b</i> , Å	8.8471 (6)	16.0396 (7)
<i>c</i> , Å	13.6309 (8)	10.3863 (5)
<i>V</i> , Å <sup>3</sup>	961.9 (2)	1281.6 (2)
<i>Z</i>	4	8
<i>d</i> <sub>calcd</sub> , mg m <sup>-3</sup>	1.75	1.60
<i>μ</i> , mm <sup>-1</sup>	0.98	0.69
<i>λ</i> , Å	0.71073	0.71073
temp, K	293	293
<i>R</i> <sub>F</sub> <sup>a</sup> obsd; all	0.040; 0.062	0.030; 0.039
<i>R</i> <sub>w</sub> <sup>b</sup> obsd; all	0.045; 0.050	0.037; 0.039

$${}^a R_F = \sum ||F_o| - |F_c|| / \sum |F_o|. \quad {}^b R_w = [\sum w(|F_o| - |F_c|)^2 / \sum w|F_o|^2]^{1/2}.$$

Table II. Fractional Atomic Positional Parameters and *B*<sub>iso</sub> Values for C<sub>6</sub>H<sub>4</sub>S<sub>2</sub>N<sup>+</sup>Cl<sup>-</sup>·SO<sub>2</sub> (3<sup>+</sup>Cl<sup>-</sup>·SO<sub>2</sub>) (ESD's in Parentheses)

atom	<i>x/a</i>	<i>y/b</i>	<i>z/c</i>	<i>B</i> <sub>iso</sub> <sup>a</sup> , Å <sup>2</sup>
Cl1	0.08722 (13)	0.250	0.0928 (6)	3.64 (4)
S1	0.01587 (8)	0.09629 (7)	0.85741 (5)	3.37 (3)
N1	0.1177 (4)	0.250	0.84167 (22)	3.42 (13)
C1	-0.1769 (3)	0.1703 (3)	0.88307 (14)	2.48 (8)
C2	-0.3255	0.0898 (3)	0.90137 (17)	3.09 (9)
C3	-0.4683 (3)	0.1706 (3)	0.91884 (18)	3.31 (10)
S2	0.23670 (13)	0.250	0.28707 (7)	3.44 (4)
O1	0.1662 (3)	0.1137 (3)	0.32112 (18)	5.92 (11)
H2	-0.318 (4)	-0.024 (4)	0.9014 (18)	4.4 (7)
H3	-0.567 (4)	0.110 (3)	0.9341 (20)	4.3 (6)

<sup>a</sup> *B*<sub>iso</sub> is the mean of the principal axes of the thermal ellipsoids.

ected. The applied field was 14 kOe, and the measured susceptibility was checked for the field dependence at several temperatures.

**Magnetic Susceptibility.** A polycrystalline sample of 3<sup>+</sup> (0.1114 g) was loaded into a high-purity quartz container in a drybox. The container was capped with a connector fitted with a stopcock and then removed from the drybox and attached to the vacuum line. The sample was evacuated and back-filled with 0.5 atm of helium. The magnetic susceptibility data are included in the supplementary material.

The measured susceptibility (Figure 1) exhibits a Curie tail due to the presence of trace amounts of paramagnetic material. The data in the temperature range 4.2–20 K were fitted to the Curie–Weiss equation together with a temperature-independent term for the sample diamagnetism.<sup>10</sup> The low-temperature paramagnetism was then subtracted<sup>10,11</sup> from the measured susceptibility, to give the results shown in Figure 1 (inset).

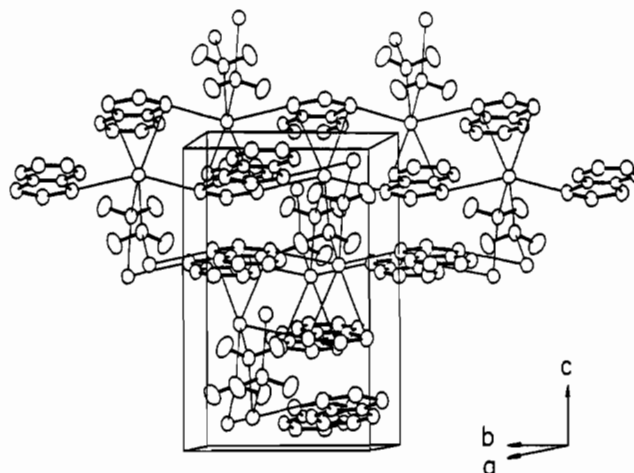
**X-ray Data Collections, Solutions, and Refinements for 3<sup>+</sup>Cl<sup>-</sup>·SO<sub>2</sub> and (3<sup>+</sup>)<sub>2</sub>.** An Enraf-Nonius CAD-4 diffractometer, equipped with graphite-monochromated Mo K $\alpha$  radiation and controlled by the NRCCAD program package,<sup>12</sup> was used to measure the unit cell dimensions and to collect the data. The crystal data are listed in Table I, and data collection details are included in the supplementary material. The unit cell constants were obtained by least-squares analysis of the diffractometer setting angles of 25 well-centered reflections by using the routine TRUANG, which centers each reflection at four equivalent positions, thereby correcting for errors in alignment. The intensities of three standard reflections were monitored and showed no significant variation in intensity during the data collection. Scattering factors<sup>13</sup> for neutral atoms were corrected for anomalous dispersion.

The structures were solved by direct methods and refined by a full-matrix least-squares procedure using anisotropic thermal parameters for all non-hydrogen atoms. The hydrogen atom positions were located from a difference Fourier synthesis and included in the final cycles of refinement with isotropic thermal parameters. The function minimized was  $\sum w(|F_o| - |F_c|)^2$ , where *w* is the weight (derived from counter statistics). No corrections were applied for absorption or extinction. All calculations

Table III. Fractional Atomic Positional Parameters and *B*<sub>iso</sub> Values for C<sub>6</sub>H<sub>4</sub>S<sub>2</sub>N<sup>+</sup> (3<sup>+</sup>) (ESD's in Parentheses)

atom	<i>x/a</i>	<i>y/b</i>	<i>z/c</i>	<i>B</i> <sub>iso</sub> <sup>a</sup> , Å <sup>2</sup>
S1	0.53856 (8)	0.51296 (3)	0.20676 (5)	3.20 (2)
S2	0.75537 (7)	0.52082 (3)	-0.00306 (5)	3.07 (2)
N1	0.6489 (2)	0.57724 (10)	0.11449 (18)	3.50 (8)
C1	0.6270 (2)	0.41883 (12)	0.15516 (20)	2.54 (8)
C2	0.7326 (2)	0.42749 (13)	0.04689 (20)	2.49 (7)
C3	0.8037 (3)	0.35722 (14)	-0.01171 (23)	3.14 (9)
C4	0.7728 (3)	0.27989 (15)	0.04135 (26)	3.42 (10)
C5	0.6705 (3)	0.27181 (13)	0.15107 (25)	3.47 (10)
C6	0.5959 (3)	0.34048 (14)	0.20769 (23)	3.19 (9)
H3	0.875 (2)	0.3627 (13)	-0.0886 (21)	2.9 (4)
H4	0.837 (3)	0.2318 (21)	-0.0002 (24)	5.2 (6)
H5	0.657 (3)	0.2181 (13)	0.1913 (20)	3.2 (5)
H6	0.521 (3)	0.3348 (15)	0.2779 (25)	3.7 (5)

<sup>a</sup> *B*<sub>iso</sub> is the mean of the principal axes of the thermal ellipsoids.

Figure 2. Contents of the unit cell of C<sub>6</sub>H<sub>4</sub>S<sub>2</sub>N<sup>+</sup>Cl<sup>-</sup>·SO<sub>2</sub> and some neighboring species.

were performed by using the NRCVAX suite of programs.<sup>14</sup> The final atomic positional parameters and isotropic temperature factors for 3<sup>+</sup>·Cl<sup>-</sup>·SO<sub>2</sub> and 3<sup>+</sup> are listed in Tables II and III, respectively.

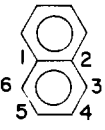
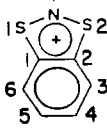
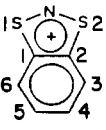
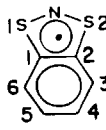
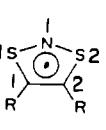
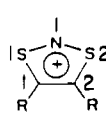
**Theoretical Methods and Geometries.** The electronic structures of 1<sup>+</sup>, 1<sup>+</sup>, 3<sup>+</sup>, 3<sup>+</sup>, and naphthalene were examined at the ab initio RHF/STO-3G (closed-shell species) and UHF/STO-3G (1<sup>+</sup> and 3<sup>+</sup>) levels<sup>15</sup> by using the Gaussian-86 suite of programs.<sup>16</sup> In order to investigate the effect of the benzo moiety on the electronic structure of the C<sub>2</sub>S<sub>2</sub>N<sup>+</sup> ring, the geometries of 3<sup>+</sup> and 1<sup>+</sup> (Table VIII) were both based on the observed structure of 3<sup>+</sup> idealized to C<sub>2v</sub> symmetry. The observed geometry of the C<sub>6</sub>H<sub>4</sub>S<sub>2</sub>N unit in (3<sup>+</sup>)<sub>2</sub> was used to represent that of monomeric 3<sup>+</sup>. This is consistent with a similar assumption recently made by Goddard et al.<sup>17</sup> and supported by the similarity of the structures of CF<sub>3</sub>CNSN<sup>+</sup><sup>18</sup> and S<sub>3</sub>N<sub>2</sub><sup>+</sup><sup>19</sup> as monomers and as parts of dimers. The geometry of naphthalene was that observed experimentally.<sup>20</sup>

The results of CNDO/2 calculations<sup>21a</sup> also carried out on these

- (11) DiSalvo, F. J.; Menth, A.; Waszczak, J. V.; Tauc, J. *Phys. Rev.* **1972**, *B6*, 4574.  
 (12) Le Page, Y.; White, P. S.; Gabe, E. J. NRCCAD, An Enhanced CAD-4 Control Program. Presented at the Annual Meeting of the American Crystallographic Association, Hamilton, Ontario, Canada, 1986.  
 (13) *International Tables for X-ray Crystallography*; vol. IV, Kynoch Press: Birmingham, England, 1974; Vol. IV.

- (14) Gabe, E. J.; Le Page, Y.; Charland, J.-P.; Lee, F. L.; White, P. S. *J. Appl. Crystallogr.*, in press.  
 (15) Hehre, W. J.; Radom, L.; Schleyer, P. v. R.; Pople, J. A. *Ab Initio Molecular Orbital Theory*; Wiley: New York, 1986.  
 (16) Frisch, M.; Binkley, J. S.; Schlegel, H. B.; Raghavachari, K.; Martin, R.; Stewart, J. J. P.; DeFrees, D.; Seeger, R.; Whiteside, R.; Fox, D.; Fluder, E.; Pople, J. A. Gaussian 86. Department of Chemistry, Carnegie-Mellon University, Pittsburgh, PA, 1986.  
 (17) Cordes, A. W.; Goddard, J. D.; Oakley, R. T.; Westwood, N. P. C. *J. Am. Chem. Soc.* **1989**, *111*, 6147.  
 (18) Hofs, H.-U.; Bats, J. W.; Gleiter, R.; Hartmann, G.; Mews, R.; Eckert-Maksie, M.; Oberhammer, H.; Sheldrick, G. M. *Chem. Ber.* **1985**, *118*, 3781.  
 (19) Gillespie, R. J.; Kent, J. P.; Sawyer, J. F. *Inorg. Chem.* **1981**, *20*, 3784 and references therein.  
 (20) Ponomarev, V. I.; Filipenko, O. S.; Atovmyan, A. L. *Sov. Phys.—Crystallogr.* **1976**, *21*, 215.  
 (21) (a) Dobosh, P. A. *QCPE* **1969**, *11*, 141. Modified by F. Grein, of University of New Brunswick, Fredericton, Canada. (b) Haddon, R. C.; Wasserman, S. R.; Wudl, F.; Williams, G. R. *J. Am. Chem. Soc.* **1980**, *102*, 6687. Haddon, R. C.; Trucks, G. W. Private communication.

**Table IV.** Comparison of Bond lengths (Å) and Angles (deg) in 3<sup>+</sup>, 3\*, and Related Heterocycles<sup>a</sup>

						
	<i>b</i>	Cl <sup>-</sup> SO <sub>2</sub> <sup>c</sup>	Br <sup>-</sup> /Br <sub>3</sub> <sup>-d</sup>	<i>c</i>	R = CF <sub>3</sub> <sup>e</sup>	R = CH <sub>3</sub> , H <sup>f</sup>
S1-N1		1.598 (2)	1.475 (10)	1.644 (2)	1.634 (4)	1.612 (7)
S2-N1		1.598 (2)	1.731 (10)	1.648 (2)	1.634 (4)	1.589 (7)
S1-C1		1.708 (2)	1.700 (5)	1.741 (2)	1.749 (5)	1.679 (7)
S2-C2		1.708 (2)	1.704 (5)	1.746 (2)	1.749 (5)	1.670 (8)
C1-C2	1.421 (2)	1.411 (5)	1.395 <sup>g</sup>	1.394 (3)	1.324 (14)	1.399 (10)
C2-C3	1.423 (2)	1.405 (3)	1.395 <sup>g</sup>	1.393 (3)		
C3-C4	1.377 (2)	1.365 (4)	1.395 <sup>g</sup>	1.378 (4)		
C4-C5	1.411 (2)	1.405 (3)	1.395 <sup>g</sup>	1.391 (4)		
C5-C6			1.395 <sup>g</sup>	1.374 (4)		
C6-C1				1.391 (2)		
S1-N1-S2		116.6 (2)	117.6 (4)	113.9 (1)	117.3 (9)	112.2 (4)
N1-S1-C1		99.1 (1)	99.6 (4)	99.4 (1)	96.5 (12)	102.3 (4)
N1-S2-C2		99.1 (1)	95.9 (4)	99.1 (1)	96.5 (12)	101.4 (4)
S1-C1-C2		112.6 (2)	115.3 (2)	112.9 (2)	114.8 (6)	110.4 (6)
S2-C2-C1		112.6 (2)	111.4 (2)	113.1 (2)		113.7 (6)
C1-C2-C3	119.05 (2)	120.5 (2)	120.0 <sup>g</sup>	120.1 (2)		
C2-C3-C4	120.25 (2)	118.0 (2)	120.0 <sup>g</sup>	119.1 (2)		
C3-C4-C5	120.5 (2)	121.6 (2)	120.0 <sup>g</sup>	120.6 (2)		
C4-C5-C6				120.8 (2)		
C5-C6-C1				119.0 (2)		
C6-C1-C2				120.4 (2)		

<sup>a</sup>Atom numbering is listed differently in literature references, and numbers have been adjusted for easy comparison. <sup>b</sup>Reference 20. <sup>c</sup>This work. <sup>d</sup>Reference 26. <sup>e</sup>Reference 2a. <sup>f</sup>Reference 2c. <sup>g</sup>Benzene ring treated as a rigid body.<sup>26</sup>

systems (with the same geometries) did not differ significantly from those obtained at the STO-3G level. The molecular orbitals generated by the CNDO/2 calculation on 1<sup>+</sup> (R = H), with the geometry shown in Table VIII, were essentially identical with those of a similar calculation that used the observed geometry of 1<sup>+</sup> (R = Me, H)<sup>2c</sup> (see Table IV). The electronic structures of these systems therefore appeared to be insensitive to small changes in geometry. The molecular orbitals generated by calculations using the STO-3G\* basis set<sup>21b</sup> did not differ significantly from those obtained at the STO-3G level.

The electronic structure of 4 was studied at the RHF CNDO/2 level, as a model for (3<sup>+</sup>)<sub>2</sub> (geometry in Table VIII).<sup>22</sup> The effect on the total energy of the system of moving the nitrogen atoms in 4 either toward or away from the inversion center (i.e. varying the angle between the C<sub>2</sub>S<sub>2</sub> and SNS planes) was also studied at this level in order to rationalize the nonplanarity of the rings observed in (3<sup>+</sup>)<sub>2</sub> (Figure 5). In a comparative study, the total energy of the monomer 1<sup>+</sup> was computed (by UHF CNDO/2) by varying the angle between the C<sub>2</sub>S<sub>2</sub> and SNS planes. Calculations on the cis conformer were attempted but did not converge.

The theoretical conclusions drawn in the paper should be viewed not as a definitive statement but as a qualitative interpretation of the bonding trends consistent with the geometries obtained from the X-ray data.

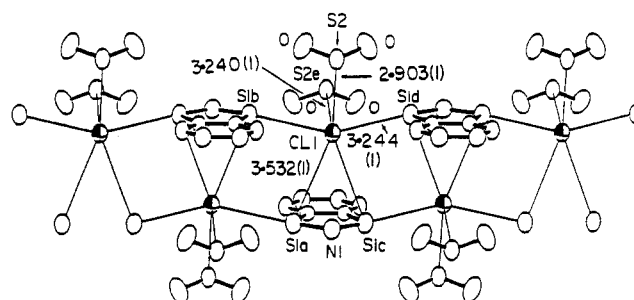
## Results and Discussion

**Crystal Structure of 3<sup>+</sup>Cl<sup>-</sup>SO<sub>2</sub>.** The structure of 3<sup>+</sup>Cl<sup>-</sup>SO<sub>2</sub> consists of discrete C<sub>6</sub>H<sub>4</sub>S<sub>2</sub>N<sup>+</sup> cations, chloride anions, and SO<sub>2</sub> molecules weakly bound together by a network of sulfur-chlorine contacts. The bond lengths and angles within 3<sup>+</sup> are given in Table IV, cation-anion contacts, distances, and angles are given in Table V, and parameters for SO<sub>2</sub> are given in Table VI. The contents of the unit cell and some neighboring species are shown in Figure 2. Figure 3 shows a portion of a ribbonlike strand along the *b* axis, made up of parallel-planar 3<sup>+</sup>, and Cl<sup>-</sup>, and some interacting SO<sub>2</sub> molecules. The two S...Cl contacts approximately in the plane of the cation [S1b...Cl1 = 3.244 (1) Å] are shorter than the two perpendicular to the plane [S1a...Cl1 = 3.532 (1) Å].

**Table V.** Interionic Contacts<sup>a,b</sup> (Å) and Selected Angles (deg) for C<sub>6</sub>H<sub>4</sub>S<sub>2</sub>N<sup>+</sup>Cl<sup>-</sup>SO<sub>2</sub>

S1a-Cl1	3.532 (1)	N1-S1a-Cl1	73.30 (11)
S1b-Cl1	3.244 (1)	N1-S1a-Cl2	163.83 (11)
		C1-S1a-Cl1	79.13 (7)
		C1-S1a-Cl2	95.22 (8)
		S1a-Cl1-S1c	45.29 (1)
		S1a-Cl1-S2e	108.66 (3)
		S1a-Cl1-S2	153.47 (2)
S2e-Cl1	3.240 (1)	S1a-Cl1-S1b	77.60 (1)
		S1b-Cl1-S2e	71.08 (2)
S2-Cl1	2.903 (1)	S1b-Cl1-S2	85.05 (2)
		S1b-Cl1-S1d	141.64 (4)
		S1b-Cl1-S1c	120.84 (3)
		S1a-Cl1-S1d	120.84 (3)
		S2e-Cl1-S2	83.91 (4)
		Cl1-S2-Cl1	144.59 (4)
		Cl1-S2-O1	97.84 (10)
		Cl1-S2e-O1	100.25 (10)

<sup>a</sup>All contacts less than the sum of the isotropic van der Waals radii of S and Cl (3.50 Å)<sup>23</sup> are included. <sup>b</sup>See Figure 3 for numbering of atoms.

**Figure 3.** Portion of a strand of (C<sub>6</sub>H<sub>4</sub>S<sub>2</sub>N<sup>+</sup>Cl<sup>-</sup>)<sub>n</sub> with interacting SO<sub>2</sub> molecules.

However, the perpendicular S...Cl contacts are only 4.5% less than the sum of the anisotropic van der Waals radius of sulfur (1.96 Å)<sup>23</sup> and the isotropic van der Waals radius of chlorine (1.76

(22) (a) The RHF method has also been employed in calculations on other loosely bound dimers, such as (NO)<sub>2</sub>,<sup>22b</sup> (NO)<sub>2</sub>,<sup>22c</sup> (S<sub>3</sub>N<sub>2</sub>)<sub>2</sub>,<sup>22d</sup> and (CF<sub>3</sub>CN<sub>2</sub>)<sub>2</sub>,<sup>18</sup> (b) Ritchie, J. P. *J. Phys. Chem.* **1983**, *87*, 2466. (c) Ahlrichs, R.; Keil, F. *J. Am. Chem. Soc.* **1974**, *96*, 7615. (d) Gleiter, R.; Bartetzko, R.; Hofmann, P. *Z. Naturforsch.* **1980**, *35B*, 1166.

**Table VI.** Comparison of Structural (Å and deg) and Vibrational Data (cm<sup>-1</sup>) for the SO<sub>2</sub> Molecule in Various Environments (Solids)

compd	av S-O	O-S-O	$\nu_{\text{asym}}$ (str)	$\nu_{\text{sym}}$ (str)	$\alpha$ (bend)
C <sub>6</sub> H <sub>4</sub> S <sub>2</sub> N <sup>+</sup> Cl <sup>-</sup> ·SO <sub>2</sub> <sup>a</sup>	1.408 (2)	117.7 (3)	1295 (vs), IR 1330 (87), R	1135 (s), IR 1124 (69), R	530 (s), IR 550 (90), R
SO <sub>2</sub> (-130 °C) <sup>b</sup> SO <sub>2</sub> (-135 °C; R) <sup>c</sup>	1.430 (15)	119.5 (1.5)	1341 (4) 1313 (10) 1310 1312	1147 (100)	524 (5)
SO <sub>2</sub> (-180 °C; IR) <sup>d</sup>				1144	528
Se <sub>2</sub> I <sub>4</sub> (AsF <sub>6</sub> ) <sub>2</sub> ·SO <sub>2</sub> <sup>e</sup>	1.39 (3)	112 (2)			
Sc <sub>6</sub> I <sub>2</sub> (AsF <sub>6</sub> ) <sub>2</sub> ·2SO <sub>2</sub> <sup>f</sup>	1.40 (2)	119 (1)	1322 (m), IR	1144 (m), IR	528 (w), IR
Te <sub>6</sub> (AsF <sub>6</sub> ) <sub>4</sub> ·2SO <sub>2</sub> <sup>g</sup>	1.41 (7)	117 (4)			
S <sub>4</sub> N <sub>4</sub> (AsF <sub>6</sub> ) <sub>2</sub> ·SO <sub>2</sub> <sup>h</sup>	1.35 (1)	122.2 (7)	1321 (s), IR	1144 (m), IR	524 (w), IR
Te <sub>2</sub> Se <sub>8</sub> (AsF <sub>6</sub> ) <sub>2</sub> ·SO <sub>2</sub> <sup>i</sup>	1.46 (7)	117 (4)			
Cs <sub>2</sub> O <sub>4</sub> ·2SO <sub>2</sub> <sup>j</sup>			1320 (s), IR	1146 (s), IR	535 (w), IR
M <sup>+</sup> SO <sub>2</sub> Cl <sup>-k</sup>			1290 (vs), IR	1120 (vs), IR	535 (m), IR

<sup>a</sup>This work. <sup>b</sup>Reference 51. <sup>c</sup>Reference 52. <sup>d</sup>Reference 53. <sup>e</sup>Reference 54. <sup>f</sup>Reference 55. <sup>g</sup>Reference 56. <sup>h</sup>Reference 57. <sup>i</sup>Reference 58. <sup>j</sup>Reference 59. <sup>k</sup>Reference 60. M = Me<sub>4</sub>N, Et<sub>4</sub>N, or n-Bu<sub>4</sub>N.

Å<sup>24</sup>), respectively, and are likely significant. They may be viewed as arising from donation from the anion into the sulfur-based LUMO of the cation (see below). In fact, the shortest Cl<sup>-</sup> contacts are to the neutral SO<sub>2</sub> molecules [S2e---Cl1 = 2.903 (1) Å, S2---Cl1 = 3.240 (1) Å] (17 and 7% less than the sum of the isotropic van der Waals radii),<sup>23</sup> which implies some SO<sub>2</sub>Cl<sup>-</sup> and/or polymeric (SO<sub>2</sub>Cl<sup>-</sup>)<sub>n</sub> character. In VSEPR terms the coordination around the sulfur atoms in SO<sub>2</sub> may be described as AEX<sub>2</sub> (SO<sub>2</sub>), AEX<sub>2</sub>Y (SO<sub>2</sub>Cl<sup>-</sup>), and AEX<sub>2</sub>YY' [(SO<sub>2</sub>Cl<sup>-</sup>)<sub>n</sub>]. The S---Cl contacts to the SO<sub>2</sub> molecules are bent away from the S-O direction [Cl1-S2-Cl1 = 144.59 (4)°], thus leaving less room than expected for the lone pair, contrary to VSEPR theory<sup>25</sup> (see Figure 3). Consequently, the O-S---Cl angles are both greater than 90° (see Table V). A total of six sulfur centers (two molecules of SO<sub>2</sub> and three cations) form contacts with each Cl<sup>-</sup> unit (Figure 3). The chlorines are in a distorted octahedral environment (Table V and Figure 3) and join the mutually perpendicular strands of (3<sup>+</sup>Cl<sup>-</sup>)<sub>2n</sub> and (SO<sub>2</sub>Cl<sup>-</sup>)<sub>n</sub>, which lie along the *b* and *a* axes, respectively (Figure 2). While the geometry of the SO<sub>2</sub> molecule is very similar to that of solid SO<sub>2</sub> and other solvated SO<sub>2</sub> systems listed in Table VI, the vibrational frequencies are intermediate between those of SO<sub>2</sub> and SO<sub>2</sub>Cl<sup>-</sup>. The solvent clearly plays a key role in the crystal lattice, as demonstrated by the difficulty in removing the solvent on evacuation and the large melting point range (129–218 °C), unlike many of the SO<sub>2</sub> solvates listed in Table VI.

The cation 3<sup>+</sup> is planar (maximum deviation of 0.035 (3) Å at N; the dihedral angle between the best planes through C<sub>6</sub>S<sub>2</sub>

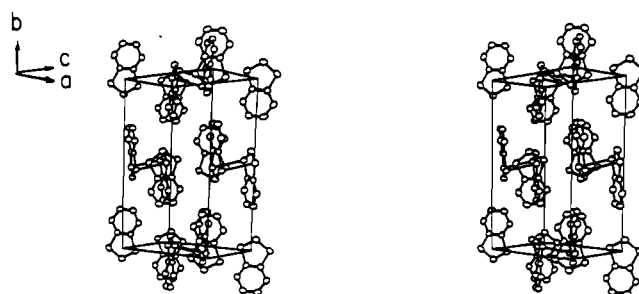


**Figure 4.** Stereoscopic view of the packing in (C<sub>6</sub>H<sub>4</sub>S<sub>2</sub>N<sup>+</sup>)<sub>2</sub> in the unit cell.

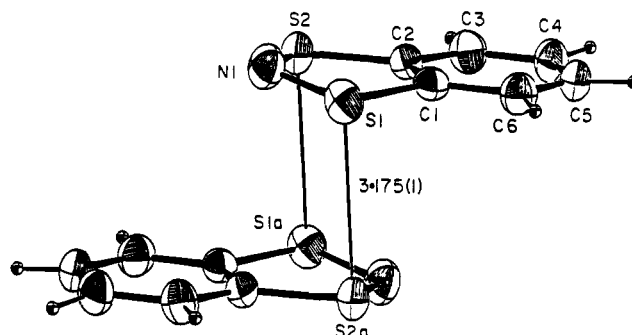


**Figure 5.** ORTEP view of the centrosymmetric (C<sub>6</sub>H<sub>4</sub>S<sub>2</sub>N<sup>+</sup>)<sub>2</sub>.

and S<sub>2</sub>N is 2.47 (22)°) and lies on a crystallographic mirror plane perpendicular to the molecular plane. In contrast, the same cation 3<sup>+</sup>, in the previously reported C<sub>6</sub>H<sub>4</sub>S<sub>2</sub>N<sup>+</sup>Br<sup>-</sup>/Br<sub>3</sub><sup>-</sup>,<sup>26</sup> exhibits severe distortion from C<sub>2v</sub> symmetry. Nevertheless, the averages of the S-N and C-S bond lengths in the Br<sup>-</sup>/Br<sub>3</sub><sup>-</sup> salt compare closely with those of the Cl<sup>-</sup> salt. The average of the bond distances and angles within the CSNSC portion of 3<sup>+</sup> are very similar to those in CH<sub>3</sub>CSNSCH<sup>+</sup>, but the C-S bond in the latter (1.674 (7) Å) is significantly shorter than that in 3<sup>+</sup> (1.708 (2) Å). Interestingly, the asymmetry present in 1<sup>+</sup> (R = CH<sub>3</sub>, H) due to the asymmetric substitution has a less pronounced effect on the heterocyclic bond lengths than does the asymmetric anion-cation contacts in 3<sup>+</sup>. Br<sup>-</sup>/Br<sub>3</sub><sup>-</sup>. The relative bond lengths in the benzo moiety of 3<sup>+</sup> are similar to the corresponding distances in naphthalene,<sup>20</sup> although slightly shorter (average C-C of naphthalene = 1.405 Å; average C-C of 3<sup>+</sup> = 1.393 Å). Thus, from a structural point of view the benzo moiety experiences a minimal effect from the replacement of the C<sub>6</sub>H<sub>4</sub> unit by SNS<sup>+</sup> (see below).

**Crystal Structure of (3<sup>+</sup>)<sub>2</sub> and a Comparison of 3<sup>+</sup> with 3<sup>+</sup>.** The structure consists of dimeric units of the bicyclic monomers bound by two long S---S contacts (3.175 (1) Å per dimer, which are

- (23) Nyburg, S. C.; Faerman, C. H. *Acta Crystallogr., Sect. B* 1985, **B41**, 274. Nyburg and Faerman derived the anisotropic van der Waals radii for the monocoordinate sulfur atoms in an R<sub>2</sub>C=S---X type environment. Although the sulfur atoms in SO<sub>2</sub>, 3<sup>+</sup>, and 3<sup>+</sup> are all dicoordinate, they do contain substantial  $\pi$  bonding, and therefore, the van der Waals radii are expected to be anisotropic. We can approximate the anisotropic van der Waals radii in these more complicated situations by using Nyburg's approach. In cases where the S-X contacts (X = Cl, S) are nearly perpendicular to the molecular plane (i.e. both C-S-Cl and N-S-Cl angles in 3<sup>+</sup>, C-S-S and N-S-S angles in 3<sup>+</sup>, and O-S-Cl angles in SO<sub>2</sub> are close to 90°), the anisotropic van der Waals radii for the sulfur atoms in these cases are likely close to Nyburg's anisotropic radius for sulfur perpendicular to the R<sub>2</sub>CS plane of 2.03 Å (cf. the isotropic van der Waals radius of S of 1.74 Å). Thus, these contacts are more significant than they appear if only the isotropic van der Waals radii had been considered. For example, the S1a---Cl1 contact at 3.532 (1) Å is above the molecular plane of 3<sup>+</sup> with C-S-Cl and N-S-Cl angles of 70° and is 5% less than the sum of the anisotropic van der Waals radius for the sulfur atom (1.96 Å) and the isotropic radii of chlorine. Similar situations are observed in the S-Cl contacts between the chloride ion and the sulfur atoms in the SO<sub>2</sub> molecules and in the interaction of the sulfur atoms between the two radicals, 3<sup>+</sup>, in the dimer. In these cases it would be reasonable to use Nyburg's anisotropic radii of 2.03 Å for sulfur. However, it is not possible to deduce the anisotropic van der Waals radii for the dicoordinate sulfur centers where the S-X contact is close to the plane of the C-S-N fragment in the molecule.
- (24) The chloride ion is not covalently bound to any other atom; therefore, the isotropic van der Waals radius of 1.76 Å is used.
- (25) Gillespie, R. J. *Molecular Geometry*; Van Nostrand-Reinhold: London, 1972.

- (26) Slawin, A. M. Z.; Williams, D. J. Department of Chemistry, Imperial College of Science and Technology, London. Unpublished results.

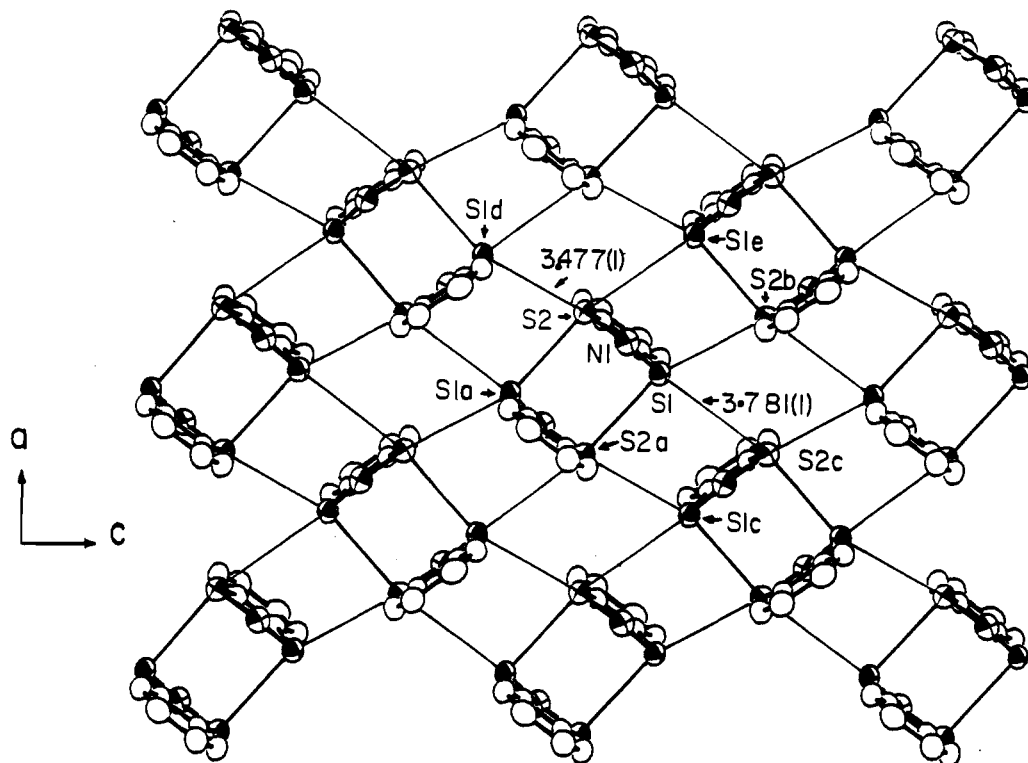


**Figure 6.** Sheets of interacting  $(C_6H_4S_2N^*)_2$  in the  $ac$  plane, as viewed along the  $b$  axis.

9% less than the sum of the isotropic van der Waals radii, 3.48 Å<sup>23,27</sup> in a parallel-planar, centrosymmetric, staggered [S1-S2-S1a = 94.17 (2)°, S2-S1-S2a = 85.83 (2)°] geometry, as illustrated in Figures 4 and 5. Each dimer has four weak contacts (3.477 (1) Å, which is equal to the sum of the isotropic van der Waals radii but is probably still significant)<sup>28</sup> to sulfur atoms in neighboring dimers, giving rise to sheets of weakly linked sulfur atoms, illustrated in Figure 6. The two-dimensional infinite structure is parallel to the  $ac$  plane at  $y = 0$  and  $1/2$ . The two sulfur atoms, S1 and S2, deviate by 0.21 and 0.49 Å, respectively, from the average plane of the sheet of centrosymmetric dimers. In addition, there are four weaker contacts between the dimers (3.781 (1) Å), which are longer than the sum of the isotropic van der Waals radii.<sup>23,28</sup> Similar interdimer interactions are observed in various  $(RCN\overline{SSN^*})_2$  structures, e.g.  $R = Ph$ ,<sup>29</sup>  $CF_3$ ,<sup>18</sup>  $NMe_2$ ,<sup>17</sup> and  $CH_3$ ,<sup>31</sup> although in these cases sheets of sulfur-sulfur contacts are not formed. Interestingly, similar S---S contacts at 3.10 Å join  $(SN)_x$  chains into sheets.<sup>30</sup> Thus, in both solid  $(3^*)_2$  and  $(SN)_x$  these weak contacts appear to have important structural consequences. The benzo moiety and two sulfur centers of the monomeric unit are planar to within 0.06 Å (the maximum deviation is 0.059 Å at C3), and the nitrogen center is removed from this plane by 0.186 (2) Å away from the partner monomer (exo with respect to the dimer unit). The angle between the planes joined by the common S-S vector is 12.05°. The distance between the  $C_6S_2$  mean planes is 3.00 Å, demonstrating a slight skew between the planes (cf. S---S = 3.175 (1) Å). The interplanar (S---S)

**Table VII.** Selected Distances (Å) and Angles (deg) in the Sheets of Interacting  $(C_6H_4S_2N^*)_2$ <sup>a</sup>

		Intradimer	
S1-S2a	3.175 (1)	S1a-S2-N1	103.9 (10)
		S1-S2-S1a	94.17 (2)
		S2-S1-S2a	85.83 (2)
		S2a-S1-N1	96.8 (1)
		Interdimer	
S1-S2c	3.781 (1)	S2-S1-S2c	169.48 (3)
S2-S1d	3.477 (1)	S2a-S1-S2b	149.04 (3)
		S2a-S1-S2c	98.55 (2)
		S2b-S1-S2c	64.69 (2)
		S1-S2a-S1c	72.69 (2)
S1a-S2-S1e	159.35 (2)		

<sup>a</sup> See Figure 6 for numbering of atoms.

distance is very similar to those observed in related systems  $[(RCN\overline{SSN^*})_2]$ :  $R = Ph$ , 3.109 (5) Å;<sup>29</sup>  $R = CF_3$ , 2.997 (2) Å;<sup>18</sup>  $R = tBu$ , 3.073 (5) Å;<sup>2b</sup>  $R = NMe_2$ , 3.036 (1) Å;<sup>17</sup>  $R = Me$ , 3.10 Å.<sup>31</sup>  $(SNSNS^+)_2(X^-)_2$ :  $X = S_2O_6Cl$ , 3.027 Å;<sup>32</sup>  $X = AsF_6$ , 2.994 (3) Å;  $X = CF_3SO_3$ , 2.996 (2) Å;  $X = SO_3F$ , 3.030 (1) Å;  $X = S_2O_2F$ , 2.986 (1) Å<sup>19</sup>. The  $3^*$  radicals dimerize by overlap of their sulfur-based radical SOMO's (see below) in a trans centrosymmetric arrangement, similar to that observed in  $(SNSNS^+)_2(X^-)_2$  (see above). The related  $(RCN\overline{SSN^*})_2$  ( $R = Ph$ ,<sup>29</sup>  $Me$ <sup>31</sup>) adopts an eclipsed cis structure, while  $(RCN\overline{SSN^*})_2$  ( $R = CF_3$ ,<sup>18</sup>  $Me_2N$ ,<sup>17</sup>  $tBu$ <sup>2a</sup>) adopt a skewed structure in which the  $\pi^*-\pi^*$  interaction involves one S---S contact. However, calculations show that for  $(HCN\overline{SSN^*})_2$ , a model for  $(CF_3C-N\overline{SSN^*})_2$ , that the energy differences between various  $\pi^*-\pi^*$  rotamers is very small.<sup>18</sup>

The strength of these interactions are very weak as measured by dimerization energies in solution [e.g.  $(RCN\overline{SSN^*})_2$ :  $R = Ph$ ,<sup>33</sup>

(27) In this case it would be reasonable to use the anisotropic radius of sulfur as 2.03 Å (see ref 23), and therefore, the interdimer S-S contact would be ca. 22% less than twice the anisotropic radius of sulfur (4.06 Å).

(28) The interdimer S---S contacts are approximately perpendicular to the plane of the ring and the other contacts are approximately in the plane of the ring. If Nyburg's<sup>23</sup> isotropic radius of 2.03 Å is used for the perpendicular anisotropic radius and Nyburg's minimum value of 1.60 Å used for the in-plane anisotropic radius, then the interdimer contacts at 3.477 (1) and 3.781 (1) Å are 4.2% less than and 5% greater than the sum of the anisotropic radius, respectively.

(29) Vegas, A.; Perez-Salazar, A.; Banister, A. J.; Hey, R. G. *J. Chem. Soc., Dalton Trans.* 1980, 1812.

(30) Labes, M. M.; Love, P.; Nichols, L. F. *Chem. Rev.* 1979, 79, 1 and references therein.

(31) Banister, A. J.; Hansford, M. I.; Hauptman, Z. V.; Wait, S. T.; Clegg, W. J. *J. Chem. Soc., Dalton Trans.* 1989, 1705.

(32) Banister, A. J.; Clarke, H. G.; Rayment, J.; Shearer, H. M. M. *Inorg. Nucl. Chem. Lett.* 1974, 10, 647.

(33) Fairhurst, S. A.; Johnson, K. M.; Sutcliffe, L. H.; Preston, K. F.; Banister, A. J.; Hauptman, Z. V.; Passmore, J. *J. Chem. Soc., Dalton Trans.* 1986, 1465.



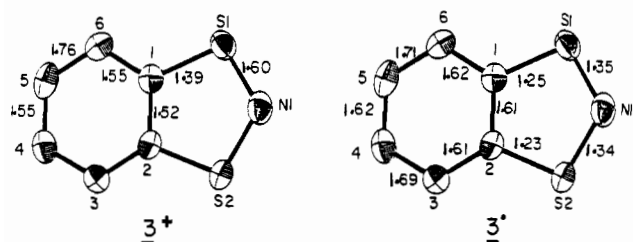


Figure 7. ORTEP views of 3<sup>+</sup> and 3\* with the corresponding empirical bond orders. (See ref 34.)

-8.8 ± 0.05 kcal mol<sup>-1</sup>; R = CF<sub>3</sub>,<sup>26</sup> -8.8 ± 0.7 kcal mol<sup>-1</sup>; R = tBu,<sup>2b</sup> -9.5 ± 0.4 kcal mol<sup>-1</sup>. For CF<sub>3</sub>CSNSCCF<sub>3</sub><sup>2b</sup> the value is zero]. The skew arrangement of the planes is also observed in related centrosymmetric structures, and it is likely that the observed equilibrium structure arises from a balance of the weak covalent, electrostatic, and van der Waals forces.

Bond lengths and angles for the monomeric unit 3\* are presented in Table IV and are compared with those of related heterocycles. Some inter- and intradimer bond distances are given in Table VII. Aside from the slight distortion from planarity, the structural features of the heterocycle are very similar to those observed in

the gas-phase structure of CF<sub>3</sub>CSNSCCF<sub>3</sub><sup>+</sup> (1\*, R = CF<sub>3</sub>). However the benzo moiety of 3\* effects a small but significant lengthening of the C-C bond in comparison to that of 1\*. Small but significant differences are observed in the heterocyclic bond distances and angles of 3\* and 3<sup>+</sup>. Both S-N and C-S bonds are longer in 3\*, while the C-C cross-ring bond is shorter. There is extensive delocalization of π bonding in both 3<sup>+</sup> and 3\* (bond orders<sup>34</sup> are given in Figure 7), but as expected, the total bond order is about 0.5 greater in 3<sup>+</sup> than in 3\*. The bond angles in 3<sup>+</sup> and 3\* are very similar, except that the SNS angle in 3\* (113.9 (1)°) is smaller than that in 3<sup>+</sup> (116.6 (2)°) consistent with longer S-N distances in 3\* (averages: 3<sup>+</sup>, 1.598 (2) Å; 3\*, 1.640 (2) Å). However, SN bond distances in 3<sup>+</sup> and 3\* imply calculated SNS bond angles of 120.3 and 93.7°, respectively,<sup>35</sup> suggesting that, in contrast to 3<sup>+</sup>, 3\* is substantially strained (see below).

**Magnetic Susceptibility of C<sub>6</sub>H<sub>4</sub>S<sub>2</sub>N<sup>+</sup> (3\*).** Figure 1 (inset) shows the molar susceptibility of 3\* from 0 to 350 K. It is apparent that three distinct temperature regions may be distinguished from the behavior of the susceptibility. Below about 160 K the break in the susceptibility suggests a phase transition, perhaps with some tendency to unpair the coupled electrons. The low-temperature Curie behavior below 20 K may arise from trace amounts of paramagnetic impurities or from small amounts of free 3\* radicals still present in the sample. If the low-temperature Curie behavior is ascribed to free spins in the sample material, then the magnitude of the signal would suggest that about 0.25% of the radicals have remained in the monomeric form.

Between 160 and 340 K the sample is diamagnetic, as would be expected of dimerized species. The measured diamagnetism corresponds to χ<sub>M</sub> = -49 emu/mol, whereas the empirical Weiss correction scheme gives χ<sub>M</sub> = -93 emu/mol. If the empirical Weiss<sup>36</sup> correction scheme reflects reality, then μ<sub>eff</sub> = 0.31 μ<sub>B</sub>.

(34) The SN bond order is calculated by Nyburg's equation:

$$N_{sn} = 0.429 + 6.85l_{sn} - 3.825l_{sn}^2$$

where  $N_{sn}$  is the SN bond order and  $l_{sn}$  the observed bond length in angstroms (Nyburg, S. C. *J. Cryst. Mol. Struct.* 1973, 3, 331). The C-C and C-S bond orders are calculated by Pauling's equation:

$$N = 10^{D_1 - D_2/0.71}$$

where  $N$  is the bond order,  $D_1 = 1.54$  and  $1.81$  Å for a C-C and C-S bond, respectively, and  $D_2$  is the observed bond length in angstroms. (Pauling, L. *The Nature of the Chemical Bond*, 3rd ed.; Cornell University: Ithaca, NY, 1960).

(35) Banister et al. have shown that the S-N bond distance ( $d_{SN}$ ) in picometers is related to the SNS bond angle ( $N$ ) in degrees, for cations and neutral species, by  $d_{SN} = 187.03 - 0.2263N$  and  $d_{SN} = 176.96 - 0.1383N$ , respectively; Banister, A. J.; Gorrell, I. B.; Roberts, R. S. *J. Chem. Soc., Faraday Trans.* 1985, 2, 1783.

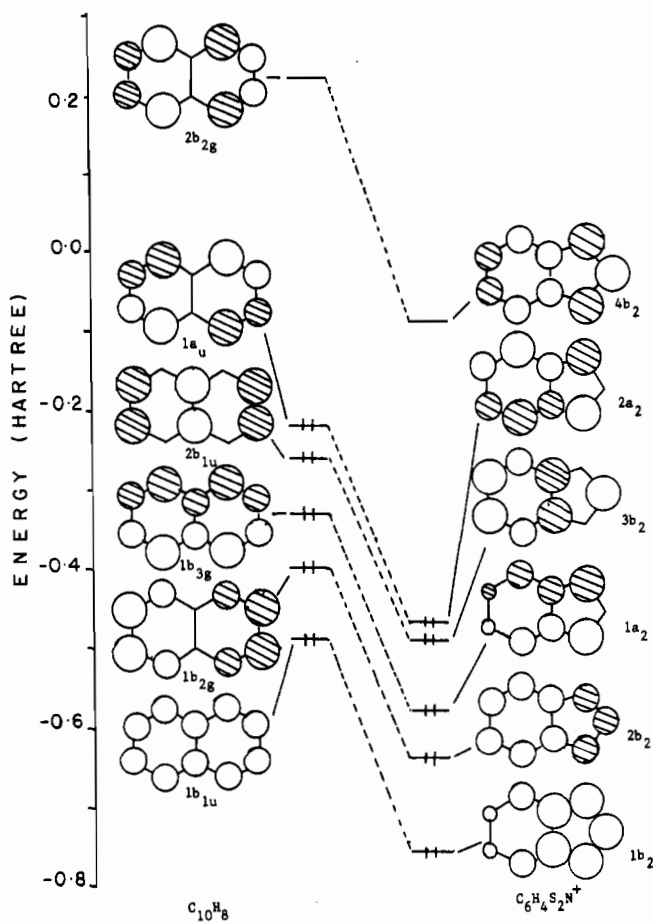


Figure 8. Comparison of the π-electronic structures of naphthalene and 3<sup>+</sup>.

Some other compounds that contain π\*–π\* dimers are also slightly paramagnetic on applying the Weiss correction scheme [e.g. (S<sub>3</sub>N<sub>2</sub><sup>2+</sup>)<sub>2</sub>(AsF<sub>6</sub><sup>-</sup>)<sub>2</sub> (χ<sub>m</sub> = 0.69 μ<sub>B</sub>)<sup>37</sup> (I<sub>2</sub><sup>2+</sup>)<sub>2</sub>(AsF<sub>6</sub><sup>-</sup>)<sub>2</sub> (χ<sub>m</sub> = 0.98 μ<sub>B</sub>),<sup>38</sup> S<sub>2</sub>I<sub>4</sub><sup>2+</sup>(AsF<sub>6</sub><sup>-</sup>)<sub>2</sub> (χ<sub>m</sub> = 0.77 μ<sub>B</sub>)<sup>38</sup>]. On the other hand, most of the analogous disulfides (e.g. (RCN<sub>2</sub>S<sup>+</sup>)<sub>2</sub>, R = CF<sub>3</sub>,<sup>39</sup> tBu<sup>2b</sup>) are diamagnetic as solids. Above 340 K there is a rapid rise in the susceptibility (see Figure 1), indicative of dissociation of the material into free radicals. The paramagnetism reaches a maximum at 360 K (mp 358–360 K), and at this temperature the magnetic moment corresponds to χ<sub>m</sub> = 1.54 μ<sub>B</sub> (on the basis of experimentally measured sample diamagnetism). Above this temperature the susceptibility of the sample decreases, presumably as a result of decomposition processes (the magnetic behavior of the material is irreversible above about 340 K). The paramagnetism of the liquid is comparable to that observed for related systems (e.g. 1\*, R = CF<sub>3</sub>; 2\*, R = tBu)<sup>2b,39</sup> in which there is no decomposition and for which the extrapolation value of the paramagnetism in infinitely dilute solution is about 1.95 μ<sub>B</sub>.<sup>2b,39</sup> Therefore, we categorize 3\* as a *paramagnetic liquid*.

**Heteronaphthalenic Nature of 3\*.** The energies and forms of the π molecular orbitals of 3<sup>+</sup> and naphthalene are shown in Figure 8. Both have five occupied orbitals, but those of 3<sup>+</sup> are lower in energy largely because of its positive charge. The forms of the molecular orbitals in the rings are similar (allowing for their

(36) Weiss, A. *Magnetochemie*; Verlag Chemie: Weinheim, Germany, 1973; pp 78–79. Values for diamagnetism correction (10<sup>-6</sup> cm<sup>3</sup> mol<sup>-1</sup>): (two S + N), -42.55; four H atoms, -8; six ring C atoms, -44.16; increment due to benzene ring, -15.10; increment for three C=C, +16.50. Sum = -93.31 × 10<sup>-6</sup> cm<sup>3</sup> mol<sup>-1</sup>.

(37) Kent, J. P. Ph.D. Thesis, Department of Chemistry, McMaster University, Hamilton, Ontario, Canada, 1984.

(38) Murchie, M. P. Ph.D. Thesis, Department of Chemistry, University of New Brunswick, Fredericton, NB, Canada, 1986.

(39) Schriver, M. J. Ph.D. Thesis, Department of Chemistry, University of New Brunswick, Fredericton, NB, Canada, 1988.

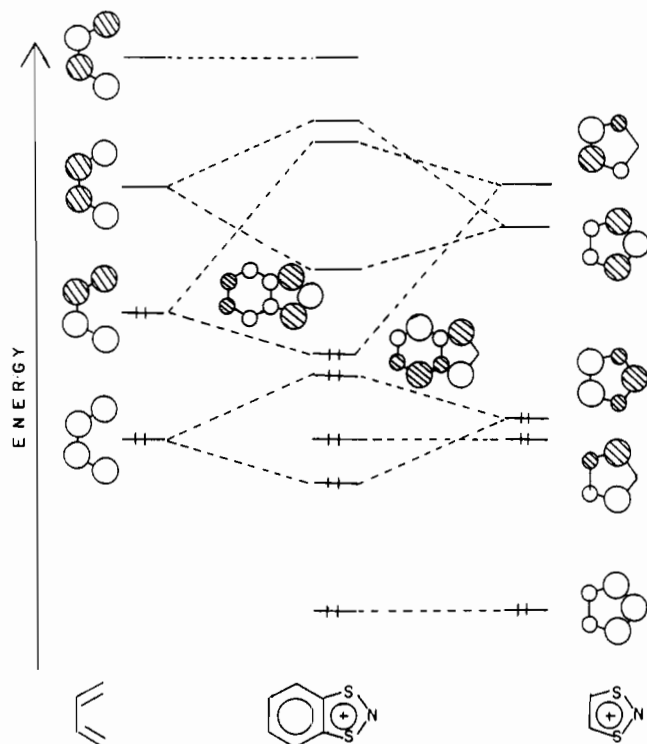


**Figure 9.** Construction of the  $\pi$  manifold of  $3^+$  from the corresponding  $\pi$  orbitals of  $C_4H_4$  and  $C_2S_2N^+$  fragments.

different point groups), and consistently the trends in C–C distances are similar in both (i.e. C3–C4 and C5–C6 shorter than C1–C2, C2–C3, C1–C6, and C4–C5). Thus,  $3^+$  may be classified as a 10- $\pi$ -electron heteronaphthalenic system, accommodating this sulfur–nitrogen-containing cation within the normal conceptual framework of organic chemistry.<sup>40,41</sup> The calculated charge distribution in  $3^+$  places a positive charge on the sulfurs (+0.6) and a negative charge on the nitrogen (–0.3), and consistently anion contacts are to sulfur but not to nitrogen.

#### Differences and Similarities in Geometries of the CSNSC Portion of $1^+$ and $3^+$ Qualitatively Accounted for by a Comparison

**of Their Electronic Structures.** The geometries of the CSNSC moiety in  $1^+$  and  $3^+$  are very similar (see Table IV) except that the C–S bond distance in  $1^+$  [1.674 (7) Å] is significantly shorter than that in  $3^+$  [1.708 (2) Å]. In order to account qualitatively for these facts, the electronic structure of the  $\pi$  orbitals in  $1^+$  are compared with those in  $3^+$  in Figure 9. The  $\pi$  orbitals in  $3^+$  have been qualitatively derived<sup>42</sup> from the corresponding orbitals in  $C_4H_4$  and  $C_2S_2N^+$  units. The major difference in the electronic structures of  $1^+$  and  $3^+$  lies in the  $3^+$  HOMO ( $2a_2$ ), the major feature of which is an antibonding C–S component and which correlates with the unoccupied, strongly antibonding  $2a_2$  MO in  $1^+$ , thus accounting for the longer C–S bond in  $3^+$ . The similarities in the geometries relate to the equivalency of the MO's of  $1^+$  with the four lower energy orbitals ( $1b_2$ ,  $2b_2$ ,  $1a_2$ ,  $3b_2$ ) of  $3^+$ .

**Comparison of the Structures of  $3^+$  and  $3^+$  and the SOMO of  $3^+$ .** The changes in bond distances that accompany the reduction of  $3^+$  to  $3^+$  are related to the phase properties of the SOMO (singly occupied molecular orbital) of  $3^+$  (see Figure 10). The largest components of this orbital are on the CSNSC portion of the ring, and bond distance changes are largest in this region. The SOMO is antibonding between S–N, C–S, and C3–C4 and bonding between C1–C2, C2–C3, and C4–C5, and consistently, the bond lengths in  $3^+$  are longer in the first set and shorter in the second set.

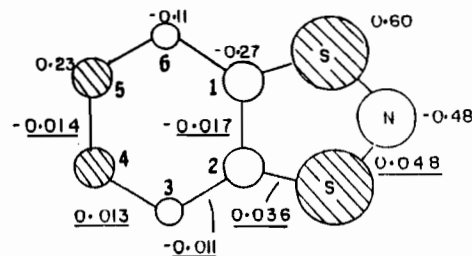


**Figure 10.** SOMO of  $3^+$  (UHF/STO-3G) with AO coefficients. Bond length changes on reduction of  $3^+$  to  $3^+$  are underlined. "+" indicates bond lengthening.

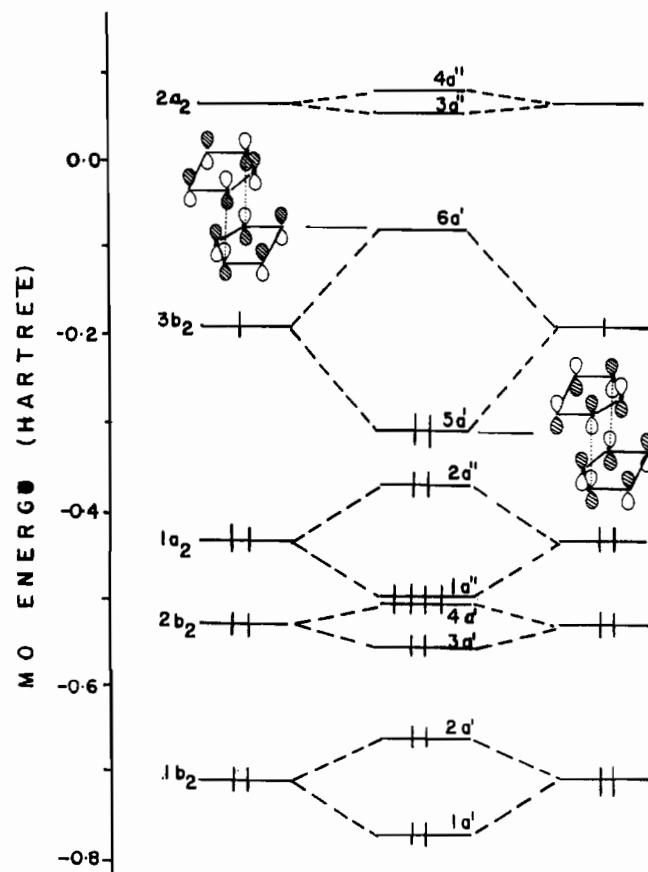


**Figure 11.** Interaction of two monomeric  $1^+$  units to give the dimer,  $4$ .

**Bonding in the Dimer ( $3^+$ )<sub>2</sub>.**  $3^+$  is observed to be weakly dimeric in the solid state. The molecular orbitals involved in dimer formation arise from the interaction of the  $\pi$  manifolds of the monomers at the sulfur centers. The dimer energy levels of  $4$  (as a model for  $(3^+)_2$ , calculated by CNDO/2; see above) are shown in Figure 11 as qualitatively arising from monomer  $\pi$  MO's (which for the purposes of Figure 11 were arbitrarily placed halfway between their corresponding bonding and antibonding dimer levels). The monomer  $1b_2$ ,  $2b_2$ , and  $1a_2$  orbitals combine to give bonding and antibonding dimer orbitals that effectively cancel one another. The  $3b_2$  SOMO's interact to give the dimer HOMO ( $5a_1$ ),<sup>43</sup> which is therefore responsible (to a first approximation) for dimer bonding.<sup>18,22d</sup> In view of this, we classify  $(3^+)_2$  as a two-center, two-electron,  $\pi^*-\pi^*$  system. A similar bonding arrangement has been proposed for  $(SNSNS^+)_{2,22d}$  and  $(CF_3-CNSSN^+)_{2,18}$  on the basis of ab initio calculations on [planar

(40) Gleiter, R. *Angew. Chem., Int. Ed. Engl.* **1981**, *20*, 444.

(41) Oakley, R. *Prog. Inorg. Chem.* **1988**, *36*, 299.

(42) Albright, T. A.; Burdett, J. K.; Whangbo, M.-H. *Orbital Interactions in Chemistry*; John Wiley: New York, 1985.

(43) The energy separation between the  $5a_1$  HOMO and  $6a_1$  LUMO of  $4$  (0.23 au, 6.2 eV) is very likely over estimated by this calculation in view of the small dimerization energy of  $(3^+)_2$  and related systems (<8 kcal mol<sup>-1</sup>).<sup>45</sup> Similarly, calculations on  $(HCNSSN)_{2,18}$  and  $(HSSH^+)_{2,22d}$  give HOMO-LUMO gaps of similar magnitude (ca. 5 and 7.5 eV, respectively).



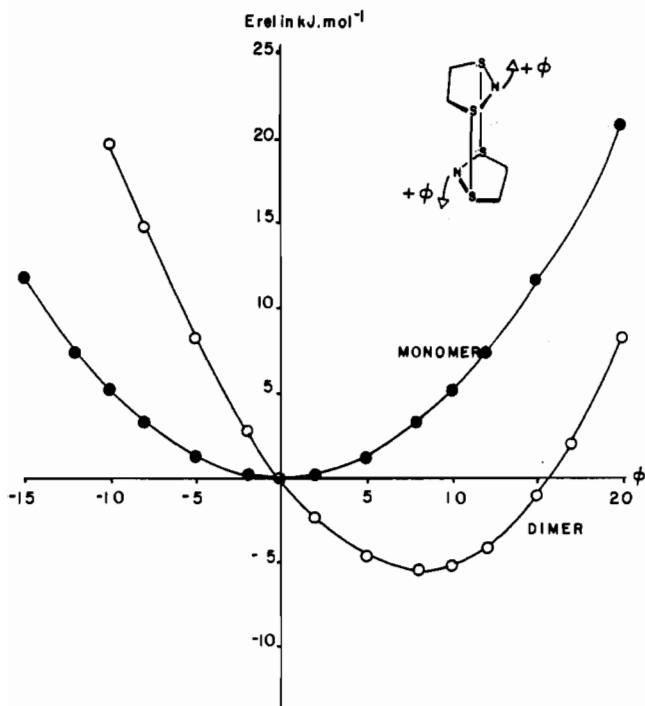


**Figure 12.** Total energies of monomer ( $1^*$ ) and dimer ( $4$ ), as a function of the angle ( $\phi$ ) between  $S_2N$  and  $S_2C_2$  planes.

**Table VIII.** Geometries Used in Calculations

parameter <sup>a,b</sup>	$1^*$ and $3^*$ <sup>c</sup>	naphthalene <sup>d</sup>	$1^*$ and $3^*$ <sup>e</sup>	$4^*/s$
point group	$C_{2v}$	$D_{2h}$	$C_{2h}$	$C_s$
S-N	1.598		1.646	1.646
C-S	1.708		1.744	1.744
$C_1-C_2$	1.405	1.421	1.392	1.392
$C_2-C_3$	1.405	1.423	1.392	
$C_3-C_4$	1.365	1.377	1.376	
$C_4-C_5$	1.405	1.411	1.392	
$\angle SNS$	116.6		114.0	115.0
$\angle NSC$	99.1		99.9	99.5
$\angle SC_1C_2$	112.6		113.1	113.0
$\angle C_1C_2C_3$	120.5	119.0	120.3	
$\angle C_2C_3C_4$	118.0	120.3	119.0	
$\angle C_3C_4C_5$	121.5	120.7	120.7	

<sup>a</sup> Bond lengths in Å and angles in degrees. <sup>b</sup> All C-H bonds were set at 1.09 Å, and angles involving the same C-H bond were set equal; e.g.  $\angle SC_1H = \angle C_2C_1H = 123.4^\circ$  in  $1^*$ . <sup>c</sup> Based on the experimental geometry of  $3^+Cl^-SO_2$  (see Table IV). <sup>d</sup> Experimental geometry. <sup>e</sup> Based on the experimental geometry of  $(3^*)_2$ . See Table IV and text. <sup>f</sup> S...S distance of 3 Å. <sup>g</sup> This geometry was also used as the basis for the conformational study on  $4$ . The N atoms were moved out of their respective  $C_2S_2N$  planes, first toward one another (negative  $\phi$ ) and then away from one another (positive  $\phi$ ). The inversion center was maintained throughout, and  $-15^\circ < \phi < 20^\circ$ .

*cis*- $H_2S_2^{*+} ]_2^{22d}$  and  $(HCN\overline{SSN^*})_2$ ,<sup>18</sup> respectively, and called by Gleiter<sup>22d</sup> a six-electron four-center bonding arrangement. This mode of bonding is therefore likely to be responsible for the weak bonding between monomers in all the various  $(RCN\overline{SSN^*})_2$  and  $(RCSN\overline{SCR^*})_2$  dimers as well as in  $(I_2^{*+})$ ,<sup>44</sup>  $(I_4^{2+})$ , and a variety of related species.<sup>45</sup>

**Nonplanarity of  $3^*$  in  $(3^*)_2$ .**  $(3^*)_2$  contains nonplanar  $C_6H_4S_2N$  units, with the nitrogen atoms bent out of the  $C_2S_2$  planes by  $12^\circ$

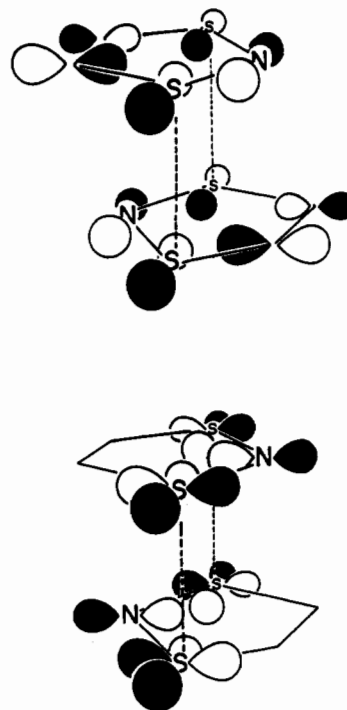


**Figure 13.** Orbitals that may be involved in S...S interdimer contacts in the solid state.

(see Figure 5). This contrasts with the planar structure of  $1^*$  ( $R = CF_3$ )<sup>2a</sup> in the gas phase. With a view to rationalizing this unusual feature the total energies of  $1^*$  ( $R = H$ ) and  $4$  were calculated for conformers of varying angle between the  $SNS$  and  $C_2S_2$  planes ( $\phi$ ) (geometries in Table VIII). Figure 12 shows the total energies (relative to planar structures),  $E_{rel}$ , of these systems as a function of  $\phi$ . Both curves are parabolic, with minima at  $E_{rel} = 0$ ,  $\phi = 0^\circ$ , for the monomer and  $E_{rel} = -5.3$  kJ/mol,  $\phi = 8.5^\circ$ , for the dimer.<sup>46</sup>

While detailed quantitative arguments are unjustified at such a low calculational level, these results can be discussed in terms of the qualitative trends that they exhibit.<sup>47</sup> The shallowness of the monomer curve (Figure 12) is indicative of a highly deformable  $C_2S_2N$  ring. This is consistent with the recent electron diffraction results for  $1^*$  ( $R = CF_3$ )<sup>2a</sup> which show the nitrogen to have a high thermal parameter in the direction perpendicular to the ring. This probably demonstrates the competing effects of ring strain (see above), which is reduced as  $\phi$  increases, and  $3p(S)\pi-2p(N)\pi$  overlap, which is a maximum at the planar configuration. The flexibility of the  $C_2S_2N$  ring is evident in the trans-parallel dimer structure  $4$ , for which the energy minimum is a geometry with the nitrogen atoms pushed out of the monomer planes away from the region of the intermolecular S...S bonds (by bond-bond repulsion), consistent with the observed structure of  $(3^*)_2$ .

**Solid-State Dimer-Dimer Interactions.** The contacts between  $(3^*)_2$  dimers to give sheets of sulfur contacts may be tentatively assigned to interactions between  $\pi$  and  $\sigma$  orbitals in the frontier orbital region. Our CNDO calculations on  $4$  imply that there exist high-lying occupied (e.g. the HOMO - 3) and low-lying unoccupied (LUMO + 1)  $\sigma$  orbitals of suitable symmetry for donation into the LUMO or from the HOMO of a neighboring dimer (Figure 13). The energy differences between the sets of orbitals are rather similar (HOMO - 3  $\rightarrow$  LUMO,  $\Delta E = 0.39$  au, 10.7 eV; HOMO  $\rightarrow$  LUMO + 1,  $\Delta E = 0.37$  au, 10.1 eV),

(44) Gillespie, R. J.; Kapoor, R.; Faggiani, R.; Lock, C. J.; Murchie, M.; Passmore, J. J. *Chem. Soc., Chem. Commun.* **1983**, 8. Faggiani, R.; Gillespie, R. J.; Kapoor, R.; Lock, C. J. L.; Vekris, J. E. *Inorg. Chem.* **1988**, 27, 4350.

(45) Burford, N.; Passmore, J.; Saunders, J. C. P. The Preparation, Structure and Energetics of the Homopolycyclic Cations of Groups 16 and 17. In *From Atoms to Polymers, Isoelectronic Analogies*; Liebman, J. F., Greenberg, A. Eds.; VCH Publishers, Inc.: New York, 1989; Chapter 2, p 53 and references therein.

(46) These figures refer to the calculations on the structures whose geometries were based on that of  $3^*$ . When similar calculations were carried out with geometries based on  $1^*$  ( $R = CF_3$ ), the monomer curve was virtually unaffected. The dimer curve maintained its overall shape but exhibited a minimum at  $E_{rel} = 6$  kJ mol<sup>-1</sup>,  $\phi = 8^\circ$ . When the S...S distance in the dimer was fixed at 3.175 Å, the curve showed a minimum at  $E_{rel} = -4$  kJ mol<sup>-1</sup>,  $\phi = 7^\circ$ .

(47) Pople, J. A.; Beveridge, D. L. *Approximate Molecular Orbital Theory*; McGraw-Hill: New York, 1970.

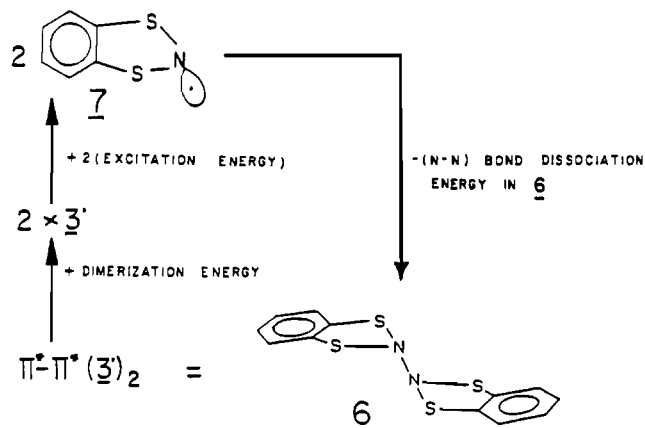
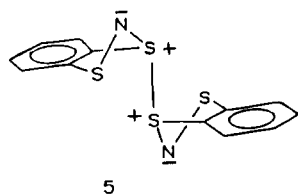


Figure 14. Energy cycle for the formation of **6** from the dimer  $(3^*)_2$ .

therefore the calculation does not suggest the direction in which donation is preferred. It is possible that both interactions occur.

**Thermodynamic Stability of the  $\pi$ -Bonded  $(3^*)_2$ .** The dimer  $(3^*)_2$  is thermodynamically more stable than alternative structures in which the monomers are joined by either an  $S^+-S^+$   $\sigma$  bond, **5**, or an  $N-N$   $\sigma$  bond, **6** (included in Figure 14). The  $N-N$



$\sigma$ -bond strength ( $35-45 \text{ kcal mol}^{-1}$ )<sup>48</sup> is likely greater than that of  $S^+-S^+$  ( $66 \text{ kcal mol}^{-1}$  in  $HSSH$ )<sup>49</sup> due to the electrostatic repulsion of the adjacent charged sulfur atoms. Therefore, the energy change between  $(3^*)_2$  and **6** may be depicted by the energy cycle in Figure 14, in which the excited-state **7** is half of **6**, with the unpaired electron localized on the nitrogen center. Then

$$\Delta H = 2(\text{excitation energy}) + \text{dimerization energy} - \text{N-N bond dissociation energy in } \mathbf{6}$$

(48) Huheey, J. E. *Inorganic Chemistry*, 3rd ed.; Harper International: New York, 1983; p A38.

(49) Schmidt, M. W.; Truong, P. N.; Gordon, M. S. *J. Am. Chem. Soc.* **1987**, *109*, 5217.

The excitation energy is equal to the difference in the sums of the bond energies of **3\*** and **7**, approximately the  $\pi$ -bond energy of the  $-CSNSC-$  portion of **3\***. This approximates to half the energy of an  $NS$   $\pi$  bond per monomer unit but is greater than this due to bond delocalization (see SOMO of **3\***, Figure 10). The localized  $NS$   $\pi$ -bond energy ( $42 \text{ kcal mol}^{-1}$ )<sup>49</sup> is very similar to  $N-N$   $\sigma$ -bond energy ( $35-45 \text{ kcal mol}^{-1}$ ). Observed dimerization energies in related dimers in solution are very small ( $0-9 \text{ kcal mol}^{-1}$ ; see above). The dimerization energy of  $(3^*)_2$  is probably not greater than  $5 \text{ kcal mol}^{-1}$ .<sup>50</sup> Thus, the  $\pi$ -bond delocalization of the  $SN$  bond in **3\*** is critical to the stability of the observed  $(3^*)_2$  configuration. Therefore,  $(3^*)_2$  and other related parallel-planar dimer molecules and ions form  $\pi$  bonds at the expense of  $\sigma$  bonds, reminiscent of radicals of second-row elements, such as  $NO^+$ ,  $O_2$ , and the nitroxides.<sup>45</sup>

**Acknowledgment.** We thank the NSERC (Canada) for financial support, the Canadian Commonwealth Scholarship and Fellowship Committee for a graduate scholarship (S.P.), Prof. F. Grein (UNB) for invaluable discussions and patient guidance in the theoretical work and the use of his programs, Dr. D. J. Williams (Imperial College, London) for kindly supplying bond distances and angles for  $C_6H_4S_2N^+Br^-/Br_3^-$  for comparison with the present data, and Dr. C.-M. Wong for help in obtaining crystallographic figures.

**Supplementary Material Available:** Tables of thermal parameters and crystallographic data for  $C_6H_4S_2N^+Cl^-SO_2$  and  $C_6H_4S_2N^+$  and magnetic susceptibility data for  $C_6H_4S_2N$  and text detailing compound preparation (10 pages); listings of observed and calculated structure factors (18 pages). Ordering information is given on any current masthead page.

- (50) Dimerization of **3\*** was not observed by quantitative ESR spectroscopy, although concentrations of the dimerization product of **3\*** are not necessarily high because of restricted solubility (see Experimental Section): Sutcliffe, H. L. Private communication.
- (51) Post, B.; Schwartz, R. S.; Fankuchen, I. *Acta Crystallogr.* **1952**, *5*, 372.
- (52) Chen, G. S. H.; Passmore, J. *J. Chem. Soc., Dalton Trans.* **1979**, 1257.
- (53) Giguere, P. A.; Falk, M. *Can. J. Chem.* **1956**, *34*, 1834.
- (54) Nandana, W. A. S.; Passmore, J.; White, P. S.; Wong, C.-M. *Inorg. Chem.* **1990**, *29*, 3529.
- (55) Nandana, W. A. S.; Passmore, J.; White, P. S.; Wong, C.-M. *Inorg. Chem.* **1989**, *28*, 3320.
- (56) Burns, R. C.; Gillespie, R. J.; Luk, W.-C.; Slim, D. R. *Inorg. Chem.* **1979**, *18*, 3086.
- (57) Gillespie, R. J.; Kent, J. P.; Sawyer, J. F.; Slim, D. R.; Tyrer, J. D. *Inorg. Chem.* **1981**, *20*, 3799.
- (58) Boldrini, P.; Brown, I. D.; Gillespie, R. J.; Ireland, P. R.; Luk, W.; Slim, D. R.; Verkris, J. E. *Inorg. Chem.* **1976**, *15*, 765.
- (59) Awere, E. G.; Passmore, J. Unpublished results.
- (60) Burrow, D. F. *Inorg. Chem.* **1972**, *11*, 573.

## Notes

Contribution from the National Chemical Laboratory, Pune 411008, India

### The Molecular Sieve VPI-5: A Precursor to $AlPO_4-8$ <sup>†</sup>

S. Prasad and I. Balakrishnan\*

Received May 1, 1990

The present work shows that the largest pore molecular sieve VPI-5, in its as synthesized form, is a precursor to  $AlPO_4-8$ , which is obtained by calcining the former in inert atmosphere or in vacuum in the temperature range  $388-773 \text{ K}$ .

Both VPI-5 and  $AlPO_4-8$  are synthesized from identical gel compositions by using tetrabutylammonium hydroxide, *n*-di-

butylamine, or *n*-dipentylamine as a templating agent at  $423 \text{ K}$ .<sup>1-3</sup> In addition, VPI-5 can also be synthesized by using *n*-dipropylamine.

The reported differences between the syntheses of VPI-5 and  $AlPO_4-8$  are only with respect to the aging and longer crystallization period required, respectively, in the two cases. However, the procedure referred to by Grobet et al.<sup>3a</sup> eliminates steps involving aging and yields VPI-5 in a shorter crystallization period. Also, the only role of templating agents appears to be to provide the optimum pH conditions.<sup>2,4</sup> Thus, all synthesis factors are

- (1) Davis, M. E.; Montes, C.; Garces, J. M.; Crowder, C. *ACS Symp. Ser.* **1989**, No. 398, 291.
- (2) Wilson, S. T.; Lok, B. M.; Flanigen, E. M. U.S. Pat. 4 310 440, 1982.
- (3) (a) Grobet, P. J.; Martens, J. A.; Balakrishnan, I.; Mertens, M.; Jacobs, P. A. *Appl. Catal.* **1989**, *56*, L21. (b) Grobet, P. J.; et al. Unpublished work.
- (4) Davis, M. E.; Montes, C.; Hathaway, P. E.; Garces, J. M. *Stud. Surf. Sci. Catal.* **1989**, *49A*, 199.

<sup>†</sup>  $(Al_{10}P_0)_2O_2$ .